JOINT INSTITUTE FOR NUCLEAR RESEARCH
Frank Laboratory of Neutron Physics

FINAL REPORT ON THE SUMMER STUDENT PROGRAM

Small angle scattering investigations of unilamellar lipid vesicles

Supervisor:
Dr. Kuklin Alexander Ivanovich

Student:
Alina Pavlova, Russia
Voronezh State Technical University

Participation period:
July 15 – August 26

Dubna, 2018

CONTENTS

1 Introduction

Nowadays, the studying of biological membranes have a importance for the development of drug delivery methods, the study of various diseases and for understanding the mechanisms of membrane and membrane-associated proteins in conditions close to biological ones.

The biological membrane is a complex system consisting of lipids, lipoproteins and proteins. Often, when studying protein molecules, the question arises of their surroundings in the membrane, so an important part is the creation of a model system that would better imitate the biological membrane. Of the most used models at the present time are nanodiscs, bicells, micelles and vesicles.

Vesicles are the most accurate system of imitation of the cell membrane, because in a closed volume of vesicles, the protein can perform its functions for pumping cations or ions, water molecules etc. In the physiological state, the lipid environment is in the liquid-crystalline phase.

The most suitable way of studying lipid vesicles is the methods of x-ray and neutron scattering, but the method of small-angle scattering (SAS) is the most suitable for studying structural phase transitions.

2 Theoretical aspects

2.1 Small-angle scattering

Small-angle scattering (SAS) is a method to study structure and interactions of systems with the size on the order of ~10 to 1000 Å. In each of these techniques radiation is elastically scattered by a sample and the analysis on the resulting scattering pattern provide the information about sample.

We assume a plane monochromatic wave $A_0 e^{ik_0 r}$ incident at the point scattering center *O,* which generates a secondary spherical wave (Figure 1).

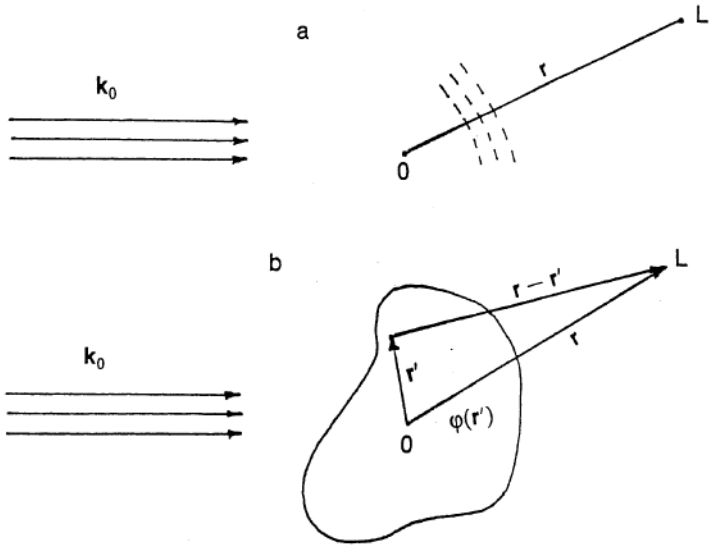

Figure 1 Scattering of a plane wave by a point scatterer (a) and a bounded potential field φ(r) (b).

Then, at some observation point, the resulting wave is given by

$$A = A_0 e^{ik_0 r} + \frac{A_0 b}{|r|} e^{ikr},$$

where k_0 and k are the incident and scattering wave vectors with $|k_0| = |k| = 2\pi/\lambda$, λ ***is*** denoting the wavelength, A_0 and $A_0 b/r$ are the scattering amplitudes of the two waves, and r is the vector which determines an observation point ***L*** corresponding to the scattering center *O*.

The stronger the interaction between the incident wave and the point center *O,* the greater the constant *b***.** This quantity has the dimension of length and is called the "scattering length", or scattering amplitude, of the center.

We consider the scattering of a plane monochromatic wave of X-rays or neutrons by a real object consisting of an accumulation of nuclei and electrons — a group of point scatterers. In this case the scattering ability of the object may be characterized by the scattering density function φ(r). This function, the potential field, is determined within a finite range of space; in some cases φ***(***r) may depend on time. In the case of X-ray scattering φ***(***r) represents the distribution of the electric charge density, while in neutron scattering these functions represents the nuclear and spin density distribution. [1]

Although the physical mechanisms of elastic X-ray and neutron scattering by matter are fundamentally different, they can be described by the same

mathematical formalism. The basics of scattering are therefore presented simultaneously, pointing to the differences between the two types of radiation. X-ray photons with an energy E have a wavelength λ = 1.256/E, where λ is expressed in nm and *E* in keV. For structural studies, relatively hard x-rays with energies around 10 keV are used (λ about 0.10–0.15 nm). The neutron wavelength is given by de Broglie's relationship, λ [nm] = 396.6/v [m s^{-1}], where v is the (group) velocity of neutrons, and thermal neutrons with wavelengths λ around 0.20–1.0 nm are typically employed. When an object is illuminated by a monochromatic plane wave with wavevector $k_0 = |\boldsymbol{k_0}| = 2\pi/\lambda$, atoms within the object interacting with the incident radiation become sources of spherical waves. We shall consider only elastic scattering (i.e. without energy transfer) so that the modulus of the scattered wave $k1 = |\boldsymbol{k1}|$ is equal to k0. The amplitude of the wave scattered by each atom is described by its scattering length, *f*. For hard x-rays interacting with electrons the atomic scattering length is $f_x = N_e r_0$ where N_e is the number of electrons and r_0=2.82 × 10^{-13} cm is the Thomson radius. The atomic scattering length does not depend on the wavelength unless the photon energy is close to an absorption edge of the atom. In this case, there is resonant or anomalous scattering, a phenomenon used for experimental phase determination in crystallography [2], and also in some SAS applications [3].

Neutrons interact with the nuclear potential and with the spin and the neutron scattering length consists of two terms $f_n = f_p + f_s$. The last term bears structural information only if the neutron spins in the incident beam and the nuclear spins in the object are oriented [4], otherwise the spin scattering yields only a flat incoherent background. In contrast to the situation with x-rays, f_p does not increase with the atomic number but is sensitive to the isotopic content. Table 1 displays two major differences between the x-ray and neutron scattering length: (i) neutrons are more sensitive to lighter atoms than x-rays; (ii) there is a large difference between the neutron scattering lengths of hydrogen and deuterium.

Atom	H	D	C	N	O	P	S	Au
Atomic mass	1	2	12	14	16	30	32	197
N electrons	1	1	6	7	8	15	16	79
f_X, 10^{-12} cm	0.282	0.282	1.69	1.97	2.16	3.23	4.51	22.3
f_N, 10^{-12} cm	−0.374	0.667	0.665	0.940	0.580	0.510	0.280	0.760

Figure 2. X-ray and neutron scattering lengths of some elements

The former difference is largely employed in neutron crystallography to localize hydrogen atoms in the crystal [4]; the latter provides an effective tool for selective labelling and contrast variation in neutron scattering and diffraction [5]. The scattering process in the first Born approximation is described by Fourier transformation from the 'real' space of laboratory (object) coordinates r to the 'reciprocal' space of scattering vectors $s=(s, \Omega) = \boldsymbol{k_1} - \boldsymbol{k_0}$. Following the properties of the Fourier transform (i.e. the reciprocity between dimensions in real and reciprocal space implying that the smaller the 'real' size, the larger the

corresponding ‘reciprocal’ size) the neutron scattering amplitudes of atoms can be considered to be constants due to the small (10−13 cm) size of the nucleus. The x-ray scattering amplitudes representing the Fourier transform of the electron density distribution in the (spherical) atom are functions $f(s)$ of the momentum transfer $s=4\pi\lambda^{-1}\sin(\theta)$ where 2θ is the scattering angle, and $f(0) = f_x$. [2]

2.3 Lipids

Lipids are a large group of natural organisms that include fats and fat-like substances. Lipids - is one of the major classes of complex molecules present in cells and tissues of the animals. The basis of the membrane are the lipids that are arranged in a bilayer.

Lipids are so-called amphipathic molecules, meaning that one molecule contains both a polar, hydrophilic head group, which tends to associate with water, and one or more hydrophobic, water repelling, tails. Due to this amphipathic character, lipids associate together in water, a process called self-assembly. The hydrophobic parts stick together, while the hydrophilic head groups are in contact with water. Dependent on the shape of the lipid and the concentration of lipids in water, different structures can form (Figure 3) [5–8], of which the lipid bilayer is a particular one. If the head group is large with respect to the hydrophobic part, the lipids will form a micelle: a globular structure in which the head groups are surrounded by water and the hydrophobic tails are sequestered inside.

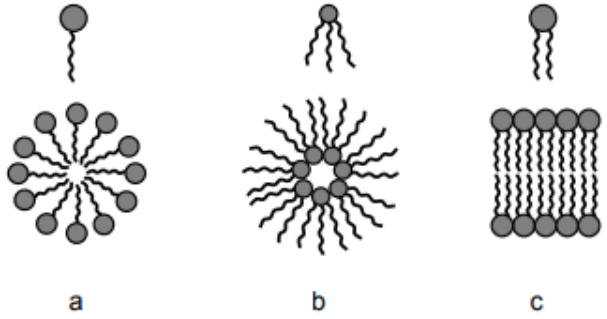

Figure 3 - Self-assembly of lipids in water gives different structures, dependent on the molecular structure of the lipid: (a) micelle, (b) inverse micelle, and (c) bilayer. The filled circles represent the hydrophilic head groups of the molecules and the wavy lines the hydrophobic tails.

The opposite is the formation of the inverse micelle, formed if the tails are bulky and the head group is relatively small. The third and most important structure in biology is the lipid bilayer. The lipids are comprised of a large head group and mostly two hydrophobic tails. This yields a roughly cylindrical molecule, which can easily pack in parallel to form extended sheets. The various structures can transform from one to another by changing the solution conditions such as the electrolyte concentration, the pH, or temperature.

The formation of lipid bilayers is a rapid and spontaneous process, with the

hydrophobic interactions as the main driving force (i.e. the hydrophobic effect). Water molecules are released from the hydrophobic tails as these tails become sequestered in the interior of the bilayer. Additionally, the vanderWaals attractive forces between the tails favor a close packing. And finally, the lipid bilayers are stabilized by the electrostatic interactions and the formation of hydrogen bonds in the head group region [9].

Membrane lipids is an amphiphilic molecule, there is, in the molecule both hydrophilic groups and aliphatic radicals forming spontaneously a bilayer (Figure 4) [10].

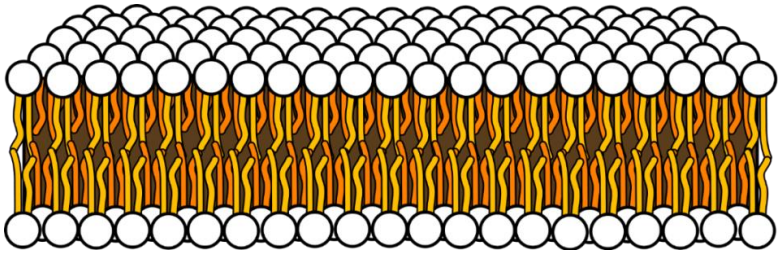

Figure 4 - Structure of the lipid membrane.

The most abundant lipids in biological membranes are the phospholipids. In figure 5 given a structure of a phospholipid .

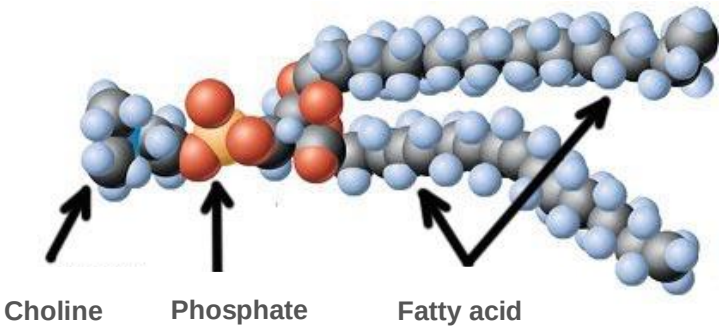

Figure 5 – General structure of phospholipids.

The backbone of a phospholipid is glycerol. To this glycerol unit two hydrocarbon tails, derived from the fatty acids, are connected. These fatty acid chains contain an even number of carbon atoms, typically between 12 and 24, of which the 16, and 18 carbon fatty acids are the most common ones. The tails can be both saturated or unsaturated, meaning that one or more double bonds between carbon atoms are present. At the remaining carbon atom of the glycerol the hydrophilic head group is attached. This head group consists of a phosphate group and an alcohol group. Different alcohols lead to a variation in head groups and thus a variation in properties of the lipid bilayer.

The bimolecular layer is shown in Figure 6. Phospholipid bilayers have a thickness of 6 to 7 nm, depending on the nature of the fatty acids contained therein. They are devoid of rigidity, since they are in a liquid state and can easily bend [2].

Vesicles (also called liposomes) are closed capsules consisting of one or more hollow objects embedded in one another, the surface of which is formed by

membrane bilayers. The internal volume of vesicles can be filled with liquid, gas, solid or dissolved material.

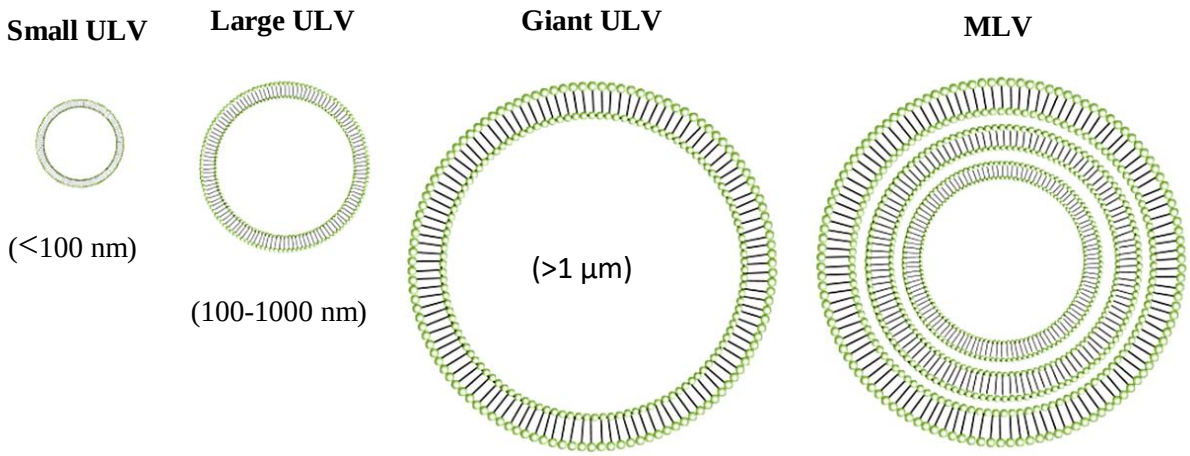

Figure 6 - Different types of vesicles: multilamellar vesicles (MLV), giant unilamellar vesicles (> 1 mm), large unilamellar vesicles (100-1000nm), small unilamellar vesicles (<100 nm).

The characteristic size of the vesicles is in the range from 200 Å to 10 μm, and the thickness of the lipid bilayer is several tens of angstroms [3].

Properties of vesicles and their behavior with the presence of a closed membrane. The lipid bilayer is distinguished by its mechanical strength and flexibility. So the vesicles change in size and shape in response to a change in the osmotic concentration of the external aqueous solution. A variety of types of vesicles are shown in Figure 6.

The use of vesicles in scientific research is associated with the modeling of cell membranes. The ability to include a variety of substances, it provides an opportunity to solve medical problems. Also, vesicles are used in the food and cosmetic industries [4].

2.4 Lipid phase transition

In the aquatic environment, the structures (Figure 7) [10] formed by phospholipids (micellar, lamellar, hexagonal, etc.) behave like liquid crystals, i.e. anisotropic fluids that have signs of order.

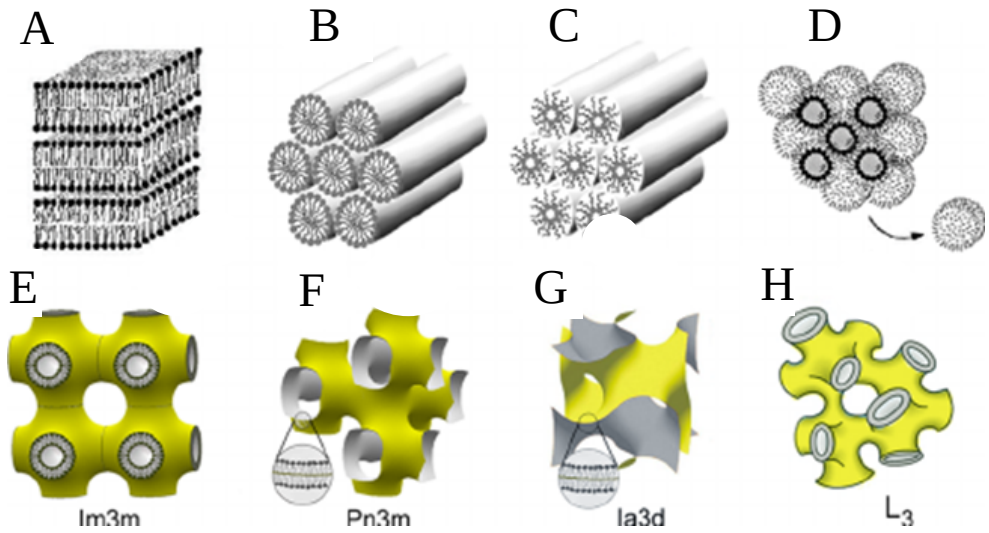

Figure7 - Structures formed in aqueous suspensions by lipids that are prone to creation: A - lamellar phase; B - hexagonal phase HI; C - inverted hexagonal phase HII; D is the inverted mycelial cubic phase of QIIM; E - bilayer cubic QII phase Im3m; F - bilayer cubic phase Pn3m; G — bilayer cubic phase Ia3d; H - sponge-like L3 phase.

Such structures are characterized by lyotropic mesomorphism (dependence of state on hydration) and thermotropic mesomorphism (dependence of structure on temperature). Both properties are related. Phase transitions of lipids, carried out by the type of "gel-liquid crystal", occur at a temperature Tcr, the value of which depends on the water content in the system. Tcr reaches a minimum as soon as the total water content exceeds the amount that can bind lipid structures. At the same time, at temperatures above Tcr, lipids with a lack of water can be in an ordered state (Figure 11).

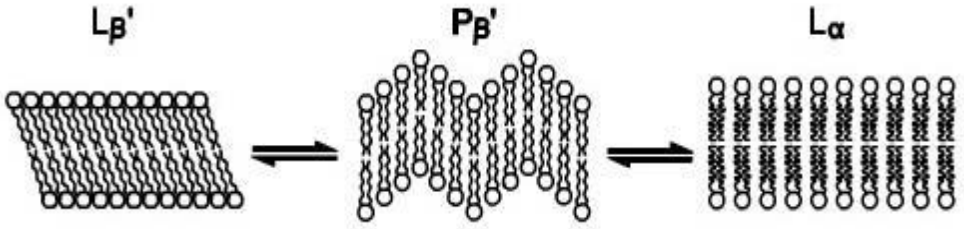

Figure 8 - Schematic representation of the three phase states of the lamellar bilayer formed by a pure phospholipid.

In the area of the phase transition, several simultaneous events occur: the mobility of the polar + N- (CH3) 3 groups increases; the rotational mobility of C – C bonds increases, which leads to the relief of gauche-trans transitions; the rate of lateral diffusion of molecules increases. The consequence of this are two important circumstances: the change in the geometric dimensions of the bilayer, due to the lateral expansion of the area occupied by each molecule of phospholipids, and an increase in the hydrophobic volume of the membrane.

The phase transitions induced by temperature are an objective characteristic of a bilayer consisting of one or several components. Phase transitions in the membrane occur not only because of temperature changes. They can also be changed by electric potential, pH shift, etc.

In addition to the transition of the “gel - liquid crystal” type, lipids can undergo transformations of another kind, leading to the formation of the hexagonal phase HII (Figure 7 B, C). These non-layered structures readily form short-chain phospholipids with polar heads (for example, phosphatidylserine, phosphatidic acid). The formation of hexagonal structures is promoted by such phenomena as an increase in temperature, an increase in unsaturation of fatty acid chains, a high ionic strength at alkaline pH, as well as a decrease in bilayer hydration. Transition of individual sections of the bilayer to the HII phase leads to disruption of the membrane integrity, the formation of permeability channels, and the formation of defective zones.

An important biological significance of phase rearrangements of the bilayer lies not only in the fact that a change in the structural state affects the change in the mobility of the components of the bilayer, the ability to regulate the interaction of membrane proteins, etc., but also that the permeability of membranes for ions in the phase transition [7].

The study of phase transitions in the lipid membrane is interesting both from a theoretical point of view [5] and from a practical one. There are several directions for the study of phase transitions by scattering methods: studies of phase transitions depending on temperature [11], studies with changes in temperature and pressure, measurements with simultaneous control of temperature, pressure and sample volume [12]. All these studies are aimed at complementing and developing the theory of phase transitions in lipid systems.

3 Materials and methods

3.1 Preparation of unilamellar vesicles

For the preparation of single-layer vesicles, the method of extruding multi-layered vesicles was used. The essence of this method is that the sample collected in the first syringe is passed through the porous membrane an odd number of times (21 times), and then the sample is removed through the second syringe. A schematic representation of the extruder is depicted in Figure 9.

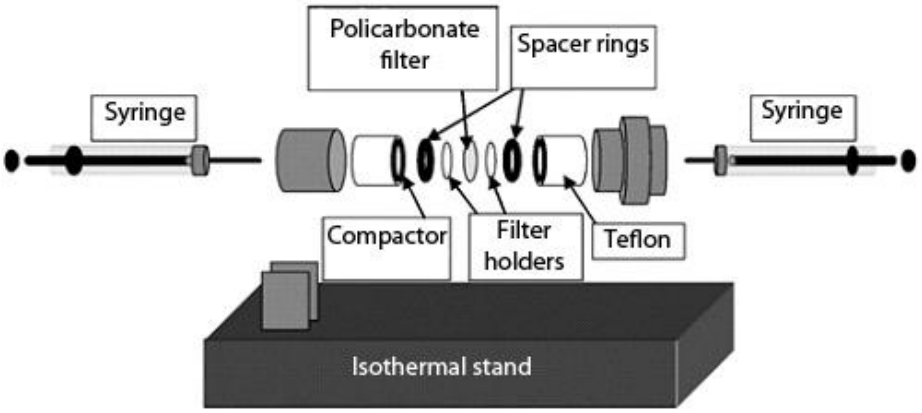

Figure 9 - Schematic representation of the extruder.

3.2 YuMO, IBR-2, BM29

Pulsed fast reactor (IBR-2) operates on the basis of the laboratory of neutron research named after. Frank (FLNP) of the Joint Institute for Nuclear Research (JINR). Neutron radiation generated by the reactor is used in more than 12 spectrometers (Figure 10), measurements of which are used in studies related to diffraction, small-angle scattering, reflectometry and inelastic scattering.

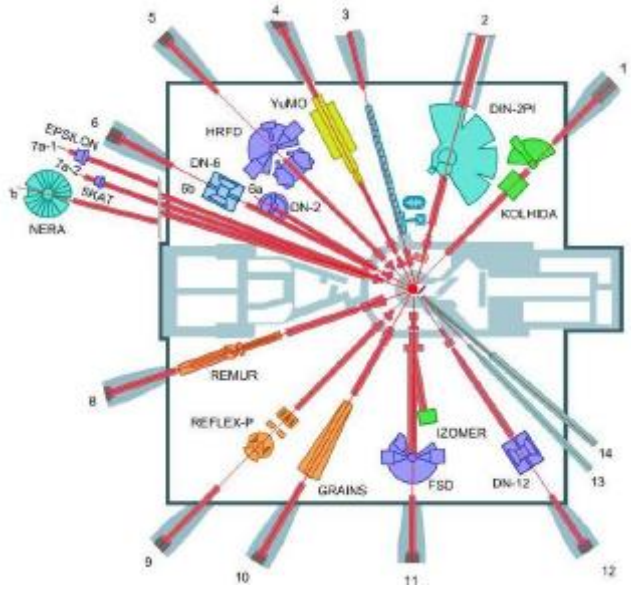

Figure 10 - IBR-2 and adjacent spectrometers.

IBR-2 has a neutron flux at the moderator ~ 1016 n / cm2 / s, with a peak power of 1850 MW. These indicators make it one of the most powerful research reactors in the world. Despite this, this reactor is environmentally beneficial: it consumes much less energy than other research reactors and uses very little fuel (less than 20 liters), which lasts about 15–20 years. Figure 11 shows the scheme of the YuMO spectrometer [13].

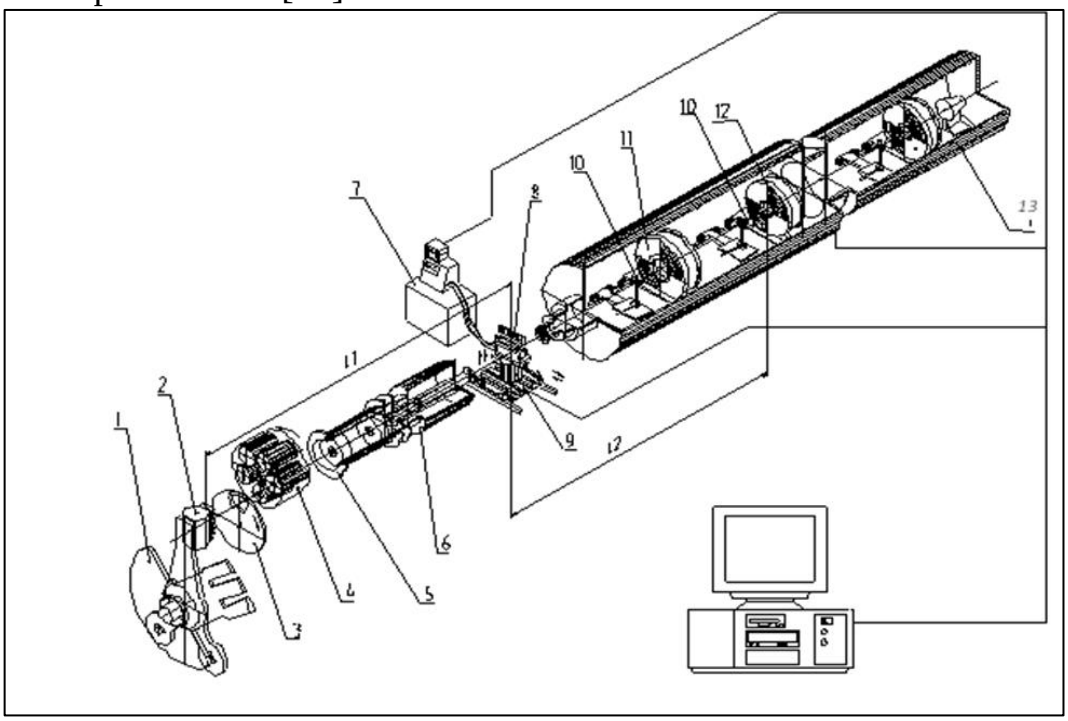

Figure 11 - Scheme of the YuMO small-angle neutron scattering spectrometer: 1 - two reflectors; 2 - reactor zone with a water moderator; 3 - breaker; 4 - the first collimator; 5 - vacuum tube; 6 - the second collimator; 7 - thermostat; 8 - removable cassette for 14 samples; 9 - sample table with thermal box; 10 - Vn standards; 11.12 - ring detectors; 13 - direct beam detector.

3.3 SasView

SasView is software for the analysis of Small-Angle Scattering (SAS) data. The software is written in Python with C and C++ modules providing some of the heavier computations.

SasView was originally developed by the University of Tennessee as part of the Distributed Data Analysis of Neutron Scattering Experiments (DANSE) project funded by the US National Science Foundation (NSF), but is currently being developed as an Open Source project hosted on GitHub and managed by a consortium of scattering facilities.

The possibilities of the SasView are listed below

- SasView fits analytic functions describing different types of material microstructure to experimental data in order to determine the shape, size and degree of ordering.
- SasView also includes tools for calculating scattering length densities, slit sizes, resolution, fringe thicknesses/d-spacings, the (Porod) invariant ('total scattering'), and distance distribution functions.

- SasView assumes that Q data is in units of /Angstroms. If your Q data is in units of /nm (or anything else) you will get incorrect parameters from your model fits. *However* if your data is in can SAS format and the Q unit is specified as /nm - ie, the XML specifies Q unit="1/nm" - SasView will internally convert the Q data to Å.
- SasView makes no assumptions about the units of I(Q) data, *but* your model fits will only return meaningful scale parameters (ie, volume fractions) if the I(Q) data is in absolute units (/cm) and on an absolute scale (ie, the I(Q) values have been calibrated against a standard).

SasView should start and present you with a screen shown in Figure 12.

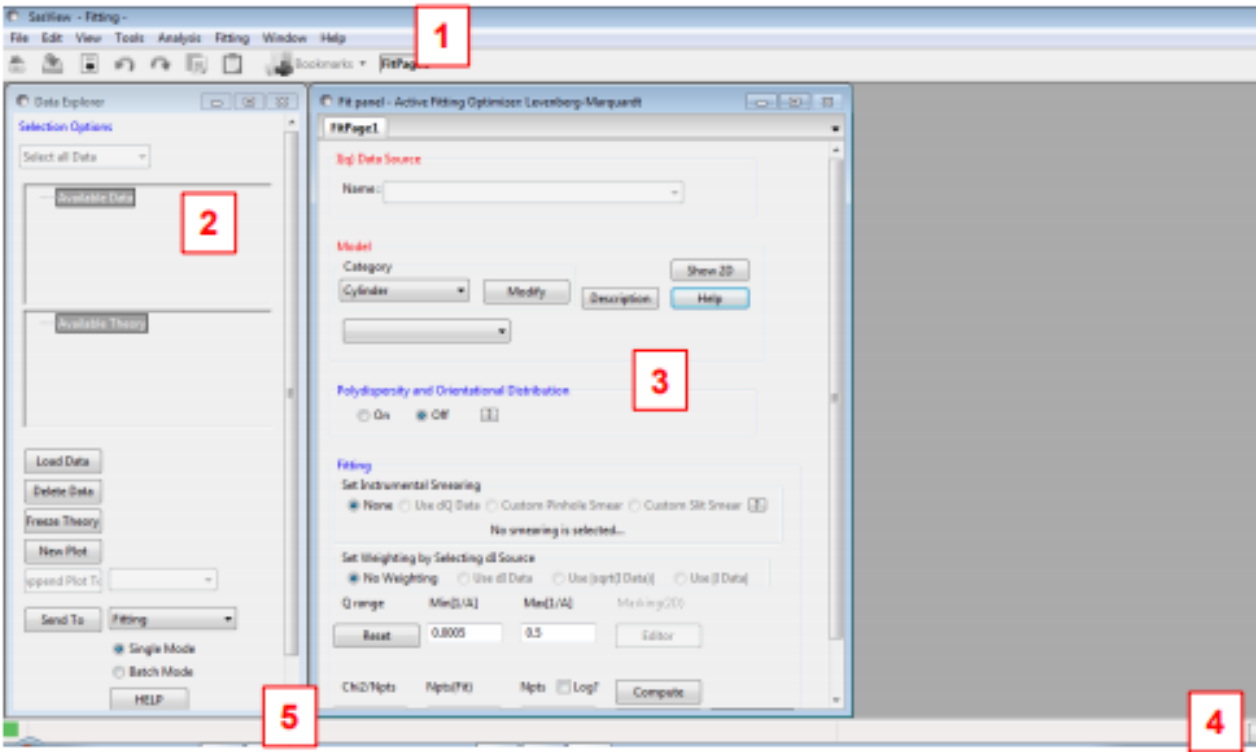

Figure 12 - Home screen of SasView

There are five elements to the initial SasView screen:

1. A Menu Bar and a Toolbar of icons
2. A Data Explorer panel
3. A Fit Page
4. The Console button
5. The Status Bar

Menu Bar / Toolbar (Figure 13), as in many other applications the Menu Bar gives access to features of the program.

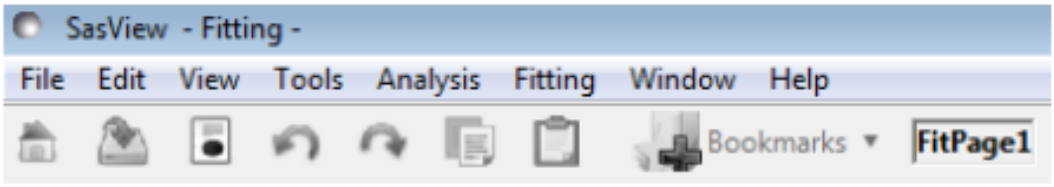

Figure 13 – SasView toolbar

File

Here you can load one of more individual data files, or an entire folder of data files into SasView. You can also save a current analysis or entire SasView session to file and then re-load them

Edit

Here you can copy/paste analysis parameters between analysis pages - useful when configuring multiple Fit Pages for, say, simultaneous fitting – or export the parameters to file.

If an analysis has been performed Report Results will prepare a report that can be saved/printed.

View

Here you can hide/show the Toolbar, the Data Explorer, and the Batch Fitting Results Panel.

Startup Setting allows you to choose whether or not SasView remembers the current configuration of the program and which folder you last loaded data from.

Category Manager allows you to re-organize the library of fitting models to your own preference.

Tools

Here you will find a collection of various utilities:

- Data Operation

Allows you to add, subtract, multiply, divide, or append two separate datasets.

- SLD Calculator

Calculates the neutron scattering length densities and electron densities of a given chemical formula.

- Density/Volume Calculator

Converts between the molar volume and mass density of a given chemical formula.

- Slit Size Calculator

Calculates the slit length for smearing purposes (as half the FWHM) from a SAXS beam profile.

- Kiessig Thickness Calculator

Calculates the Kiessig thickness from the Q-value of a fringe in a reflectivity profile, or the d-spacing from the Q-value of a peak in SAXS/SANS data, as $2\pi/Q$.

- Q Resolution Estimator

Estimates the Q-resolution of SAXS/SANS data from given instrumental

parameter values, assuming that the detector is flat and normal to the incident beam.

- Generic Scattering Calculator

Attempts to simulate the SANS expected from a specified shape/structure or scattering length density profile. The tool can handle both the nuclear and magnetic contributions to the scattering.

- Python Shell/Editor

Opens a Python 2.7 shell and editor; useful for editing and testing plug-in fitting models.

- Image Viewer

This tool loads and displays 2D SAS image data as X-Y pixel coordinates versus whatever the 'intensity' value is per pixel). The supported input image formats are: BMP (bitmap format), GIF (graphical interchange format), JPG (joint photographic experts group format), PNG (portable network graphics format), and TIF (tagged image format). The displayed 2D plot can then can be copied, printed, or re-saved as any of the above formats or as PS (postscript), EPS (encapsulated postscript), PDF (portable document format), RAW/RGBA (raw rgba bitmap), or SVG (scaleable vector graphics). If the min/max Q limits of the X-Y axes are known this tool will also convert the image to pseudo-data, for example, for 2D fitting or further manipulation.

Analysis

Here you can also select the type of analysis you wish to perform:

- Fitting

Performs optimised model-fitting on one of more datasets, with or without constraints, polydispersity or orientation distributions, or resolution smearing.

- Pr Inversion

Calculates the distance distribution function – or 'P(r) curve' - for a dataset.

- Invariant

Calculates the Porod Invariant (sometimes denoted as Q*) - or 'Total Scattering' - for a dataset.

- Correlation Function

Calculates the 1D density correlation function for a dataset. If the data is from a sample that can be described by idealised lamellar morphology this analysis will also attempt to extract some morphological information from the correlation function; eg, lamellar spacing, crystallinity, etc.

Fitting

Provides access to advanced model-fitting options. Here you can set up parameter constraints between Fit Pages or simultaneous fits, change the default fitting optimiser used by SasView, test/enable/disable fitting computations using OpenCL (a means of speeding up some complex fits by taking advantage of any high-performance graphics card processor installed in your computer), and create/manipulate/delete plug-in fitting models. [14]

4 Practical part

Phospholipids are the main components of cell membranes. Research into the structure of phospholipids is important from a viewpoint of structural biology and biochemistry. Unilamellar vesicles (ULV) are especially interesting because most biological membranes are unilamellar and properties of integral membrane proteins depend on the lipid bilayer structure at nanoscale is important for pharmacology. SAS technique is known as effective method to study the internal bilayer structure of vesicle systems.

In present work, we study ULV of DMPC and DPPC lipids of different sizes. It is known that during the phase transition, the internal radius of the vesicle is enlarged, in connection with the change in the hydration of the lipid heads and thickness of lipid membrane was decrease by increasing temperature [2].

SANS measurements were approximated by SasView. Here we can see dependences of the thickness of the bilayer and internal radius of the vesicle, as a function of temperature (Figure 14). Red curves - for a vesicle prepared with a membrane of 300 angstroms (heating process), black curves for a vesicle prepared with a membrane of 300 angstroms (cooling process), blue curves for a vesicle prepared with a membrane of 500 angstroms (heating process)

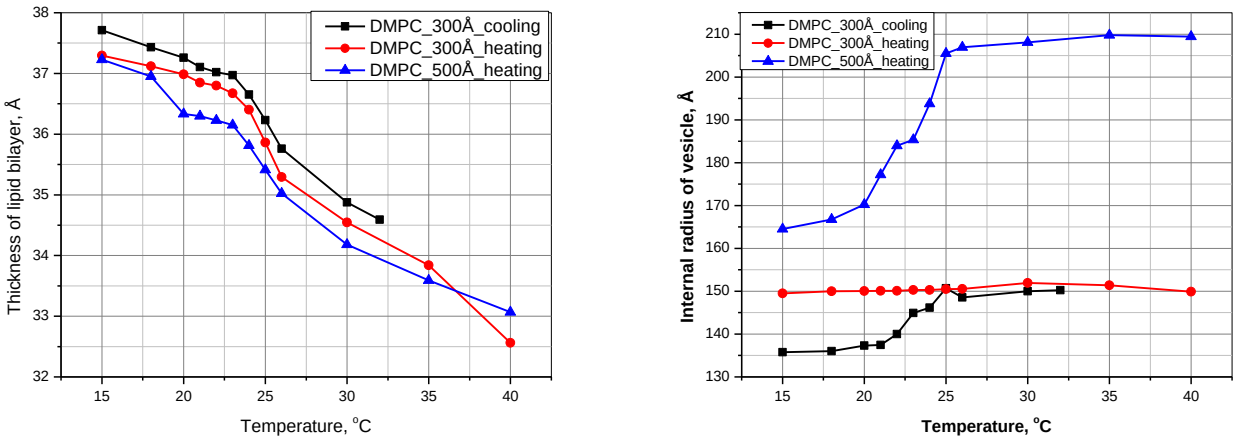

Figure 14 – dependences of the thickness of the bilayer and internal radius of the vesicle, as a function of temperature

Previously, studies were carried out. The resulting data were built according the inner radius and the thickness of the temperature. (Figure 15) We performed DMPC 300A measurements in the temperature range 18-30 °C (a), DPPC 500A in the temperature range of 20-43 °C (b) and processed the data to verify the frequency of the processes (c).

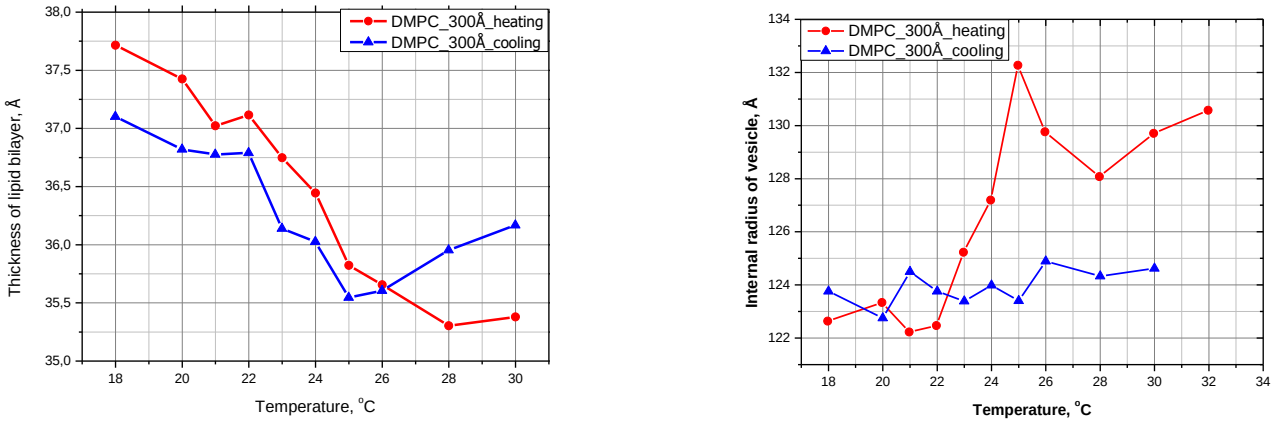

a)

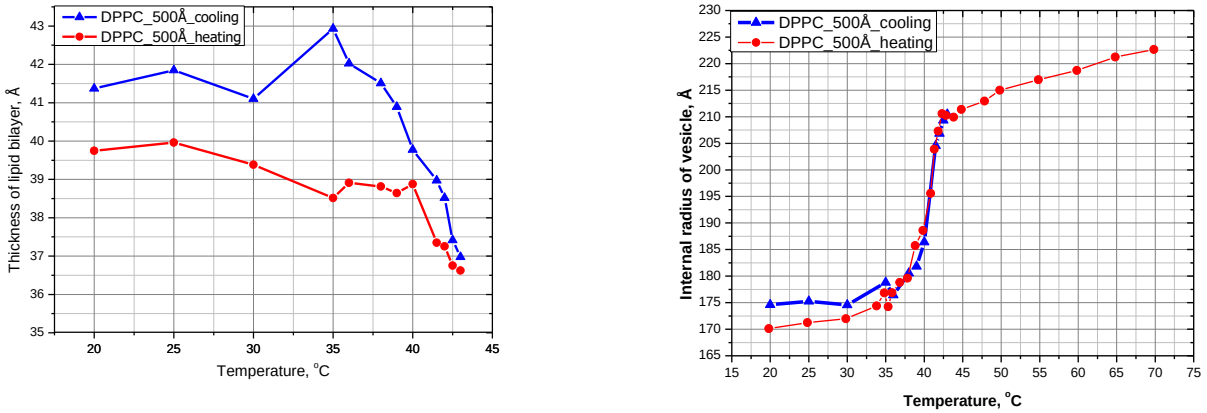

b)

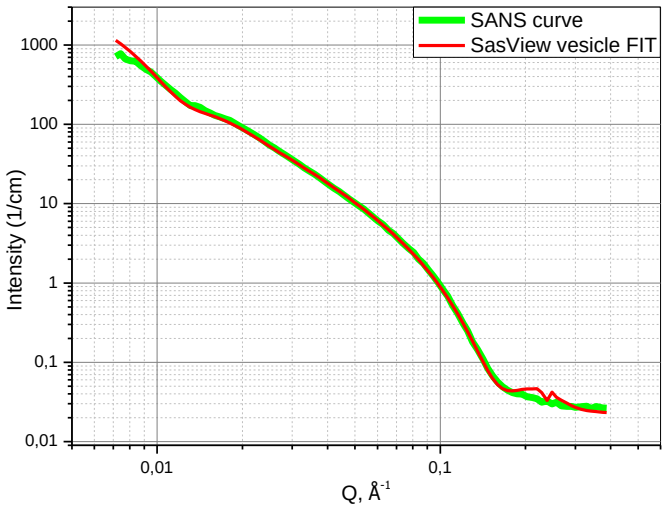

c)

Figure 15 – a) DMPC 300A in the temperature range 18-30 ºC, b) DPPC 500A in the temperature range of 20-43 ºC, c) SANS data

Based on the Figure 16, we made the assumption of lipid separation into 5 conditional layers. Using the SasView model sphere, core_multy_shell, n = 5 were fitting DMPC ULV 300A.

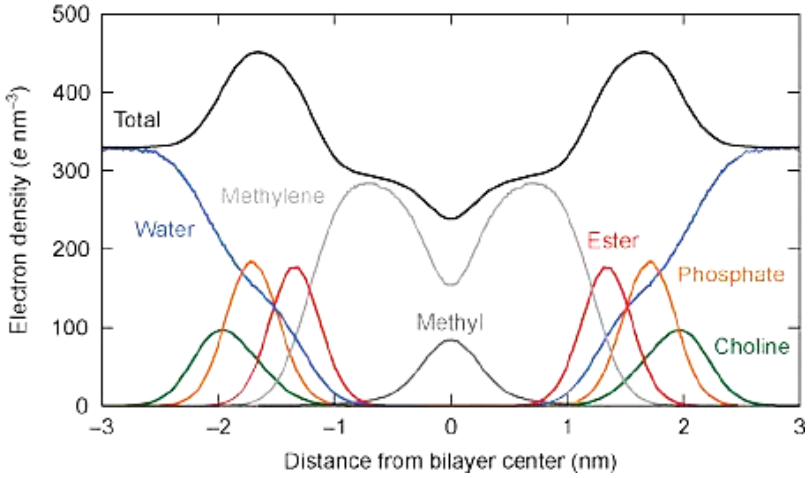

Figure 16 – dependences distance from bilayer center and electron density

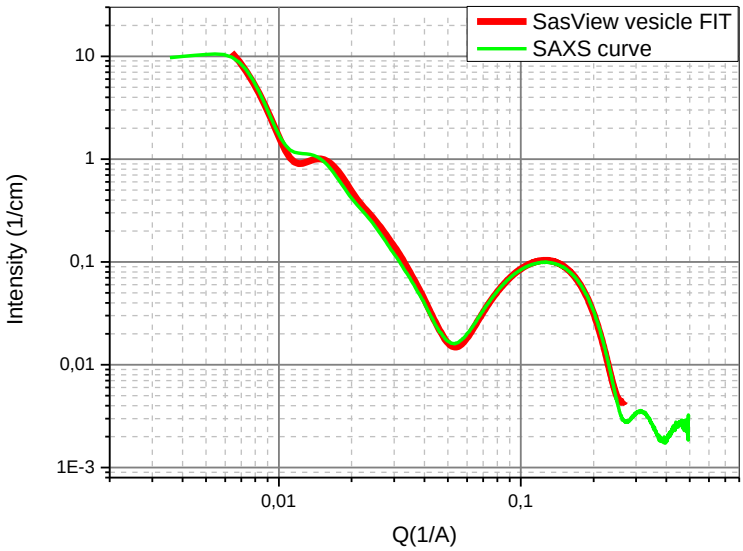

Figure 17 – SAXS data

Table 1 – Size obtained by the core multi shell model

	Bilayer						
Name of layer	**Head**	**Tail 1 part**	**Tail between**	**Tail**	**Head**	**Radius**	**Solvent**
Size, Å	**11,069**	**10,845**	**5,0708**	**10,042**	**11,562**	**204,63**	∞
SLD, $10^{-6}/Å^{2}$	**12,658**	**8,5592**	**6,1541**	**6,875**	**13,993**	**9,45**	**9,45**

5 Conclusion

In this work, we show the relationship between the size of the vesicle and the temperature phase transition using SANS and SAXS.

Obtained graphic dependences which shown the curves of SANS and SAXS measurement's, with using different form-factors. For SANS it was vesicle model, for SAXS it was core multi shell model. It was observed the relationships between inner radii and thickness of vesicles vs temperature near phase transitions.

Also, it has been found possible for a fitting SAXS data by dividing bilayer by 5 single layers with core multi shell model in SasView. This allowed to profit areas that previously could not fitted, at the same time it has been the high resolution of the method.

6 Acknowledgements

I would like to thank the University Center of the Joint Institute for Nuclear Research (JINR) for giving me the opportunity to practice at the Frank Laboratory of Neutron Physics. Special thanks should be given to YuMO head leader in FLNP Dr Alexander Kuklin, my research project supervisor for his professional guidance and valuable support.

I would also like to thank all the members of staff at Frank Laboratory of Neutron Physics, who helped me in my supervisor's absence. In particular I would like to thank PhD student of FLNP at YuMO group Maxim Rulev for his useful and constructive recommendations, for his time and valuable feedback during the investigation, for the detailed explanation theoretical part of this project and for motivation, research Assistant Vadim Skoi for the valuable technical support and for teaching practical skills on this project. I have been extremely lucky to have a Researchs who cares so much about my work, and who responded to my questions and queries so promptly.

I also wanted to thank Moscow Institute of Physics and Technology for the opportunity to conduct research on the basis of their institute.

At last I am thankful to plenipotentiary of Romania and Slovakia for material support in my research project.

References

[1] Svergun DI, Feigin LA 1986 X-ray and neutron small-angle scattering Moscow: Nauka, Ch. Ed. fiz.-mat. lit.
[2] Chantler C T et al 2003 National Institute of Standards and Technology, Gaithersburg, MD, http://physics.nist.gov/ffast
[3] Vladimirov Yu. 2000 Biological membranes and unprogrammed cell death Soros's educational journal.6 (9): 2-9.
[4] Kuklin A.I, Islamov A.K, Gordeliy V.I. 2005 Two-Detector System for Small-Angle Neutron Scattering Neutron News.16:16-18.
[5] Cullis, P. R.; de Kruijff, B. Biochim. Biophys. Acta 1979, 559, 399–420.
[6] Israelachvili, J.; Marcelja, S.; Horn, R. G. Q. Rev. Biophys. 1980, 13, 121–200.
[7] Israelachvili, J. Intermolecular & surface forces; Academic Press: San Diego, CA, 1997.
[8] Damodaran, K. V.; Merz Jr., K. M. Biophys. J. 1994, 66, 1076–1087.
[9] Alberts, B.; Johnson, A.; Lewis, J.; Raff, M.; Roberts, K.; Walter, P. Molecular Biology of the cell; Garland Science: New York, 2002
[10] Severin E. 2004 ed. Biochemistry. Textbook for High M:. Publisher GEOTAR Media.776.
[11] Ivkov V.G., Berestovsky G.N., Bergelson L.D. 1981 Dynamic structure of lipid bilayer: Science.
[12] Barsukov L. 1998 Liposomes Soros Educational Journal.10: 2-9.
[13] http://ibr-2.jinr.ru/.
[14] https://www.sasview.org/